



Earth Rotation Parameters Determination with BDS-3/LEO Simulations Under Small-Scale Ground Networks

Xinqi Fang^{1,2}, Lei Fan^{2,3}(✉), Shiwei Guo^{1,2}, Linghao Zhou^{1,2}, and Chuang Shi^{1,2}

¹ School of Electronics and Information Engineering, Beihang University,
Beijing 100191, China

xqfang@buaa.edu.cn

² Key Laboratory of Navigation and Communication Fusion Technology, Ministry of Industry
and Information Technology, Beijing 100191, China

bhflei@buaa.edu.cn

³ Research Institute for Frontier Science, Beihang University, Beijing 100191, China

Abstract. The inclusion of Low Earth Orbit (LEO) spaceborne GNSS observation or Inter-Satellite Link (ISL) measurement improves strength of normal equation, and then helps to improve ERP accuracy. With a 15-day simulation of BDS-3 ISL measurements and BDS-3 observations from 72 LEO satellites, 10 global stations and 10 Chinese stations, this work studies the impact of LEO satellites and BDS-3 ISL on ERP accuracy. Results show that the introduction of LEO satellites and BDS-3 ISL significantly improves ERP accuracy. Taking the IERS 14 C04 product as a reference, with ground network of 10 global stations, the RMS of polar X, Y coordinate and LOD after introducing 72 LEO satellites are $10.4 \mu\text{as}$, $10.8 \mu\text{as}$, $3.9 \mu\text{s}$, respectively. Compared with ERP accuracy based on solely 10 global stations, the improvement reaches 66.8%, 74.0%, 62.1%, respectively. The accuracy is equivalent to that of using 115 global stations, and the polar coordinate accuracy is better than the case of introducing BDS-3 ISL. Based on 10 Chinese stations, the RMS of polar X, Y coordinate and LOD with BDS-3 ISL are $16.3 \mu\text{as}$, $39.8 \mu\text{as}$, $7.9 \mu\text{s}$, respectively. The contribution of BDS-3 ISL is more pronounced than that of 72 LEO satellites. ERP results based on Chinese stations indicate that the polar Y coordinate accuracy is always worse than the X component, which is not found in results of global stations. Furthermore, analysis of correlation indicates that the inclusion of LEO satellites or BDS-3 ISL reduces correlation between estimated parameters.

Keywords: Earth Rotation Parameters (ERP) · Low Earth Orbit (LEO) satellite · Inter-Satellite Link (ISL) · Integrated adjustment

1 Introduction

The Earth Rotation Parameters (ERP) is a set of angles that describe irregularity of earth's rotation [1]. It consists of polar coordinates X, Y, polar motion rates, the UT1-UTC, and

© Aerospace Information Research Institute 2022

C. Yang and J. Xie (Eds.): *China Satellite Navigation Conference (CSNC 2022) Proceedings*, LNEE 910, pp. 102–112, 2022.

https://doi.org/10.1007/978-981-19-2576-4_10

its rate, the Length of Day (LOD). Since ERP is a subset of transformation parameters between the Celestial Reference System (CRS) and the Terrestrial Reference System (TRS), it plays an indispensable role in satellite orbit determination, TRF realization, and et al.

Benefited from stable constellations, and the full-weather and full-time observation capability, the Global Navigation Satellite System (GNSS) provides an efficient approach to determining ERP. Except for the GNSS's incapability in establishing UT1-UTC due to its high correlation with satellite orbit orientation elements [2]. The quality of GNSS-derived ERP are equivalent to the products derived from other space geodetic techniques [1]. Nevertheless, in traditional practices of ERP determination using GNSS technique, a large number of global ground stations are required for ensuring ERP accuracy. However, an independent large-scale global ground network is not available to most countries and regions.

In the 1990s, the US's Goddard Space Flight Center (GSFC) found for the first time that jointly processing ground-based observations and spaceborne inter-satellite measurements improves spacecraft orbit accuracy [3]. In the 2000s, Zhu et al. of the German Research Centre for Geosciences (GFZ) validated the effect of integrated adjusting ground-based observations and multiple spaceborne measurements in improving not only orbit determination but also estimation of geocenter and gravity-field coefficients. Furthermore, Zhu et al. pointed out the potential of the strategy in estimating ERP [4].

Following the pioneering researches, Svehla validated the influence of Jason-2 satellite's spaceborne GPS, DORIS data on ERP result [5]. Moreover, the Kepler system is the concept of the third generation GNSS of Europe. With simulated optical ISL and LEO spaceborne L-band observations of Kepler, Glaser et al. and Michalak et al. investigated future benefits of Kepler's new measurements to ERP determination based on 124 global observing stations. The analysis of Glaser et al. indicated that the inclusion of Kepler's new measurements improves ERP formal error [6]. Moreover, Michalak et al. showed that the new measurements mitigate the influence of perturbation force modeling deficiencies and bias on the ERP accuracy [7].

Nevertheless, how's the effect of the LEO and ISL observations on ERP determination without a perfect large-scale global ground network still remains investigated. Aims at answering this question, this study explores the impact of LEO spaceborne BDS-3 observations and BDS-3 ISL measurements on ERP estimation under two ground networks of 10 global stations and 10 Chinese stations, respectively.

1.1 Orbit Simulation

In this paper, we numerically integrate initial orbit elements to generate simulated ephemeris. The initial orbit of BDS-3 satellites come from the GBM precision ephemeris of GFZ. Furthermore, LEO satellites' initial orbit elements come from constellation design software. Design of the LEO constellation is displayed in Fig. 1. The Walker constellation consists of 72 satellites that are evenly distributed in 6 orbital planes. The phasing parameter is 1. The orbital inclination is 86.4° , the height is 1200 km, and the eccentricity is 0. Moreover, we summarize information of perturbation force model in Table 1. It is worth explaining that since initial LEO orbit elements output by the design

software lack dynamic parameters, we use a physical model based on panel information to better reflect solar radiation pressure perturbation of LEO satellites.

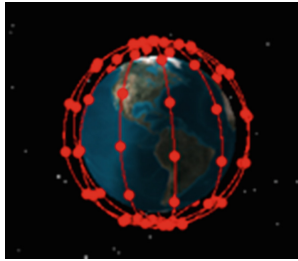


Fig. 1. Design of the LEO constellation

Table 1. Information of perturbation force models

Item	Description
N-Body	JPL DE405(Earth, Sun, Moon, Mercury, Venus, Mars, Jupiter, Saturn, Uranus, Neptune, Pluto)
Earth gravity	EGM (12 × 12) for BDS-3 and EIGEN 6C (120 × 120) for LEO
Ocean tide	FES 2004
Solid earth tide and pole tide	IERS 2010 convention
Solar radiation pressure	ECOM5 for BDS-3 and physical model for LEO
Relativity	IERS 2010 convention
Atmospheric drag	DTM94 for atmospheric density and only for LEO; Estimate Cd once per 90 min
Empirical acceleration	BDS-3: A constant term in along-track direction, and estimate it per day
	LEO: Once-per-revolution terms in along-track and cross-track direction, and estimate them per 90 min

2 Simulation Strategy

2.1 BDS-3 ISL Measurement Simulation

BDS-3 is currently the only GNSS constellation that deploys ISL. For consistency, we also simulate the inter-satellite ranging measurement between BDS-3 satellites for investigation. The scan range of the beam is set as $(-60^\circ, 60^\circ)$ with respect to nadir. The topology is “All-Connected”. It means that once two satellites in scan range are visible to each other, a link between them is built. A Gaussian noise whose standard deviation is 5cm is added to simulate ranging precision. The hardware influence is ignored.

2.2 Ground-Based and LEO Spaceborne BDS-3 Observation Simulation

Observation equations of ground-based and LEO spaceborne L-band BDS-3 observations can be expressed as follows:

$$\begin{aligned}
 P_{GND,i}^S &= \rho_{GND}^S + c \cdot (t_{GND} - t^S) + I_{GND,i}^S + T_{GND}^S + c \cdot (B_{GND,i} - B_i^S) + \varepsilon_{GND,i}^S \\
 L_{GND,i}^S &= \rho_{GND}^S + c \cdot (t_{GND} - t^S) - I_{GND,i}^S + T_{GND}^S + \lambda_i \cdot (b_{GND,i} - b_i^S) + \lambda_i \cdot N_{GND,i}^S + \omega_{GND,i}^S \\
 P_{LEO,i}^S &= \rho_{LEO}^S + c \cdot (t_{LEO} - t^S) + I_{LEO}^S + c \cdot (B_{LEO,i} - B_i^S) + \varepsilon_{LEO,i}^S \\
 L_{LEO,i}^S &= \rho_{LEO}^S + c \cdot (t_{LEO} - t^S) - I_{LEO,i}^S + \lambda_i \cdot (b_{LEO,i} - b_i^S) + \lambda_i \cdot N_{LEO,i}^S + \omega_{LEO,i}^S
 \end{aligned} \tag{1}$$

where P and L are pseudorange and phase measurement, respectively. ρ is geometric range. c is speed of light in vacuum. t is clock offset. I and T are ionospheric and tropospheric delay, respectively. Since LEO satellites are operating above troposphere, we ignore the tropospheric delay in LEO spaceborne observations. Furthermore, B and b are code and phase bias, respectively. λ is the wavelength of signal. N is ambiguity in phase measurements. ε and ω are observation noise in code and phase measurement, respectively. The subscript GND and LEO represent GNSS receiver in ground station and aboard LEO satellite, respectively. The subscript i denotes different frequencies. And the superscript S denotes different BDS-3 satellites.

Table 2. Strategy of observation simulation

Item	Description
Mask Angle	7° for ground stations and 1° for LEO satellites
Frequencies	B1 (1561.098 MHz) / B3 (1268.520 MHz)
Interval	30 s
Period	DOY 188–202, 2020
BDS-3 Clock Offset	GBM product
LEO Clock Offset	Value of ground receiver’s low-cost clock as a substitution
Ground Receiver Clock Offset	Real Precise Point Positioning (PPP) estimation
Differential Code Bias (DCB)	CAS DCB product
Phase Center Offset (PCO)	BDS-3: igs14.atx; LEO: not considered Ground stations: values of GPS as a substitution
Phase Center Variation (PCV)	Not considered
Zenith Tropospheric Delay (ZTD)	Wet: real PPP estimation; Dry: the model of Saastamoinen
Ionospheric Delay	Values from CODE GIM (Global Ionosphere Map) product
Ambiguity	Random integer that is consistent along the arc
Observation Noise	Gaussian random. Standard Deviation (STD) for code: 3 m; STD for phase: 3 mm [8]

We simulate error characteristics of ground-based and LEO spaceborne BDS-3 observations with various error corrections with the strategy in Table 2. In this study, a global

network of 10 evenly distributed global stations and a regional network of 10 evenly distributed Chinese stations are used for investigation. In addition, a large-scale global network that consists of 115 global stations is selected for comparison. The distribution of the three ground networks is displayed in Fig. 2.

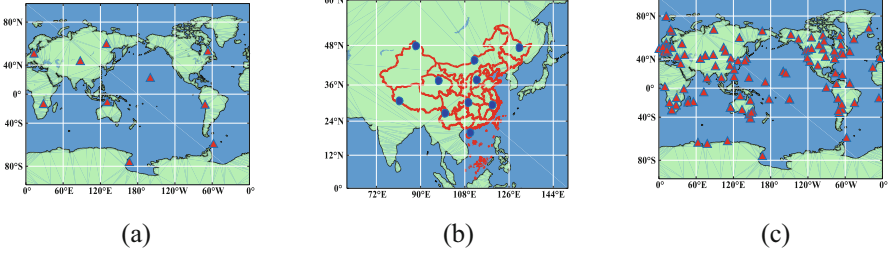


Fig. 2. Distribution of three ground networks (10 global stations, 10 Chinese Stations and 115 global stations)

3 Mathematical Model

In this study, an Ionosphere-Free (IF) combination is formed to eliminate the influence of first-order ionospheric delay in BDS-3 observations. After that, observation equations for integrated adjustment can be formulated as follows:

$$\begin{aligned}
 L_{GND} &= G(\mathbf{x}_0^S, \mathbf{x}_{GND}, \mathbf{x}_{ERP}, \mathbf{x}_{EST}, t) + \boldsymbol{\varepsilon}_{GND} \\
 L_{LEO} &= F(\mathbf{x}_0^S, \mathbf{x}_0^{LEO}, \mathbf{x}_{EST}, t) + \boldsymbol{\varepsilon}_{LEO} \\
 L_{ISL-S} &= R(\mathbf{x}_0^S, \mathbf{x}_{EST}, t) + \boldsymbol{\varepsilon}_{ISL-S}
 \end{aligned} \tag{2}$$

where $\mathbf{x}_0^S = (\mathbf{r}_0^S, \dot{\mathbf{r}}_0^S, \mathbf{p}^S)$ and $\mathbf{x}_0^{LEO} = (\mathbf{r}_0^{LEO}, \dot{\mathbf{r}}_0^{LEO}, \mathbf{p}^{LEO})$ are initial state vectors of BDS-3 and LEO satellites. In the listed-above equations of \mathbf{x}_0^S and \mathbf{x}_0^{LEO} , \mathbf{r}_0 and $\dot{\mathbf{r}}_0$ are satellite position and velocity vectors at the reference epoch. \mathbf{p} is the vector of dynamic parameters. Furthermore, \mathbf{x}_{GND} in (2) is the vector of station coordinates. \mathbf{x}_{EST} is the vector of other estimated parameters. \mathbf{x}_{EST} consists of clock offset of LEO, BDS-3 satellites and ground receivers, ZTD, ambiguity and so on. Moreover, \mathbf{x}_{ERP} is the vector of ERP. $\boldsymbol{\varepsilon}$ represents observation noise.

For ERP determination, our initial values are from IERS 14 C04 product. Furthermore, loose a priori constraints of $\sigma_{PM} = 30\text{as}$ for polar coordinate, $\sigma_{PMrate} = 3\text{as/d}$ for polar motion rate, $\sigma_{UT1} = 2\text{s}$ for UT1-UTC, and $\sigma_{LOD} = 0.2\text{s/d}$ for LOD are adopted. Partial derivatives for ERP can refer to [9]. And we estimate ERP once a day.

4 Experiment and Analysis

4.1 ERP Results Under the Ground Network of 10 Global Stations

In this study, we take the ERP data used for orbit and observation simulation as reference and estimate ERP accuracy as “recovery”. Under 10 global stations, Fig. 3 displays a 15-day time series of ERP difference with respect to the reference. The “72L”

denotes 72 LEO satellites. The “ISL” represents BDS-3 ISL. The results based on BDS-3 observations of 115 global stations are given in Table 3 for comparison.

It can be seen that LEO spaceborne BDS-3 observation and BDS-3 ISL measurement play a positive role in improving ERP accuracy. As shown in Fig. 3, when LEO satellites or BDS-3 ISL is introduced, fluctuation of time series decreases. These facts result in the pronounced improvement shown in Table 3. With LEO constellation, the RMS improvement of polar X and Y coordinate, LOD under 10 global stations reach 66.8%, 74.0% and 62.1%, respectively. The accuracy is equivalent to that of 115 global stations. Besides, the RMS improvement brought by BDS-3 ISL measurement are up to 18.2%, 49.4% and 62.1%, respectively.

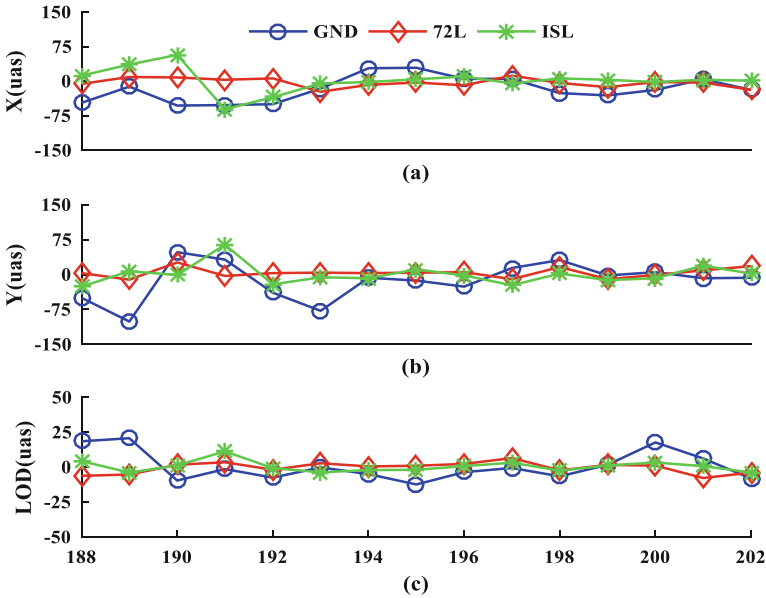


Fig. 3. Time series of the ERP difference with respect to the IERS 14 C04 product. The ground network consists of 10 global stations

Table 3. ERP RMS value with LEO spaceborne BDS-3 observations and BDS-3 ISL measurements. The ground network consists of 10 global stations

	XP (μas)			YP (μas)			LOD (μs)		
	Exp	Value	Impv	Exp	Value	Impv	Exp	Value	Impv
115GLB	GND	8.4	--	GND	11.1	--	GND	2.1	--
10 GLB	GND	31.3	--	GND	41.5	--	GND	10.3	--
	72L	10.4	66.8%	72L	10.8	74.0%	72L	3.9	62.1%
	ISL	25.6	18.2%	ISL	21.0	49.4%	ISL	3.9	62.1%

4.2 ERP Results Under the Ground Network of 10 Chinese Stations

Figure 4 plots time series of ERP difference under 10 Chinese stations. Moreover, the RMS is summarized in Table 4. It can be seen that the contribution of LEO satellites and BDS-3 ISL to ERP accuracy improvement are also significant. As shown in Fig. 4, after introducing 72 LEO satellites or BDS-3 ISL, the maximum pole coordinate difference decreases from 0.50mas to 0.25mas, and the LOD difference improves by 50%. These results indicate the effect of LEO and BDS-3 observations in improving ERP accuracy under a regional ground network.

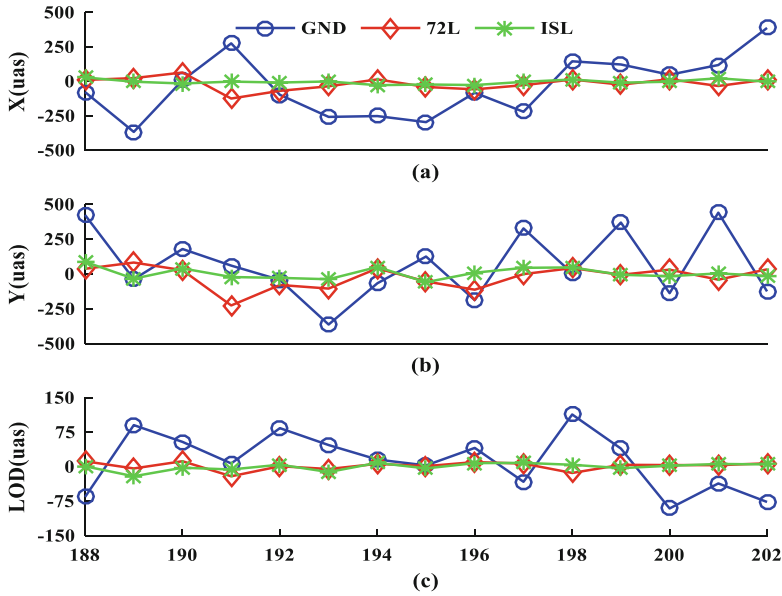


Fig. 4. Time series of the ERP difference with respect to the IERS 14 C04 product. The ground network consists of 10 Chinese stations

Table 4. ERP RMS with LEO spaceborne BDS-3 observations and BDS-3 ISL measurements. The ground network consists of 10 Chinese stations

	XP (μ as)			YP (μ as)			LOD (μ s)		
	Exp	Value	Impv	Exp	Value	Impv	Exp	Value	Impv
115GLB	GND	8.4	--	GND	11.1	--	GND	2.1	--
10 CHN	GND	216.2	--	GND	241.7	--	GND	62.0	--
	72L	48.1	77.8%	72L	81.6	66.2%	72L	9.0	85.5%
	ISL	16.3	92.5%	ISL	39.8	83.5%	ISL	7.9	87.3%

More specifically, it can be seen in Table 4 that the inclusion of 72 LEO satellites brings RMS improvement of 77.8%, 66.2% and 85.5% in terms of polar X, Y coordinate

and LOD, respectively. And the introduction of BDS-3 ISL measurement brings RMS improvement of 92.5%, 83.5% and 87.3% in terms of polar X, Y coordinate and LOD, respectively. Since the simulation ignores influences of unexpected error sources, results in this study would be more optimistic than actual cases.

Notably, polar Y coordinate accuracy is always worse than that of polar X coordinate in Table 4, which is not found in previous results of global stations. This phenomenon is also obvious in ERP estimations of Wan et al. that are based on measured GPS data of 18 Asia-Pacific regional stations and 75 global stations [9]. Since longitude range of China varies from 73°E to 135°E, the polar X-axis points to the 0° meridian and the Y-axis points to the 270° meridian, China is located on the same side of the polar X-axis. Therefore, the above phenomenon would be attributed to the regional distribution of ground network.

4.3 Correlation Analysis of Orbit Elements and ERP

In practices of ERP determination using GNSS, ERP are estimated simultaneously with orbit elements. Therefore, ERP accuracy is sensitive to the GNSS satellite orbit accuracy. To investigate the impact of LEO satellites and BDS-3 ISL on ERP accuracy, average correlation coefficients between satellite orbit elements and ERP are plotted in Fig. 5 and Fig. 6. The orbit elements include position (X, Y, Z), velocity (VX, VY, VZ), parameters of ECOM5 solar radiation pressure model (D0, Y0, B0, BC1, BS1) and empirical force (EA).

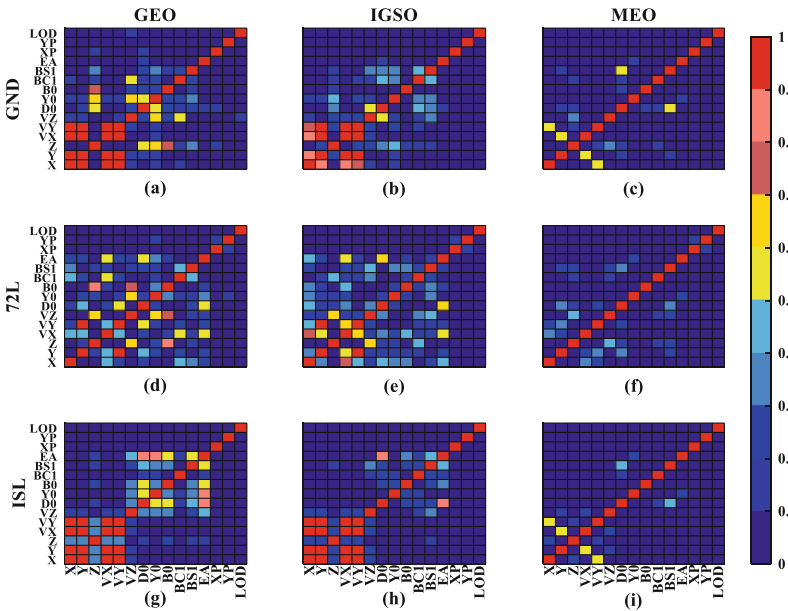


Fig. 5. Correlation analysis under 10 global stations. The ticks are X, Y, Z, VX, VY, VZ, D0, Y0, B0, BC1, BS1, EA, XP, YP, LOD

The first-row graphs with solely ground-based BDS-3 observations show that there's obvious correlation between parameters, especially under the cases of GEO and IGSO satellites. Pronounced correlation primarily exists between satellite orbit parameters. This problem would weaken the strength of normal equation, which does harm to improving ERP accuracy. Nevertheless, as shown in other graphs that introduce LEO satellites or BDS-3 ISL, the overall correlation coefficients are significantly reduced. These results indicate that LEO satellites and BDS-3 ISL observations improve strength of normal equations. This contribution would illustrate the ERP accuracy improvement in previous sections.

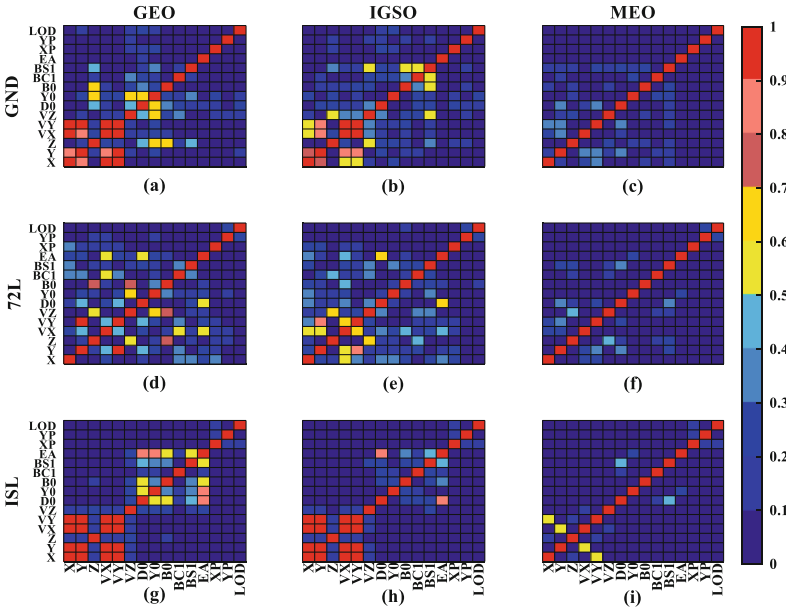


Fig. 6. Correlation analysis under 10 Chinese stations. The ticks are X, Y, Z, VX, VY, VZ, D0, Y0, B0, BC1, BS1, EA, XP, YP, LOD

5 Conclusion

Current researches on ERP determination with LEO satellites and ISL were performed with large-scale global networks. With a 15-day simulation of observations from 72 LEO satellites, 10 global stations and 10 Chinese stations, we studied the impact of LEO spaceborne BDS-3 observations and BDS-3 ISL measurement on ERP accuracy when ground network is not perfect. Notably, our results based on ground simulations of 10 global stations and 10 Chinese stations are equivalent to that from measured GPS data of 21 global stations in Wang et al. [10], and 18 Asia-Pacific regional stations in Wan et al. [9], respectively. This fact illustrates the rationality of our simulation and evaluation strategy. Our experiments indicate that:

- 1) Under 10 global stations, the RMS of polar X, Y coordinate and LOD after introducing 72 LEO satellites are 10.4 μs , 10.8 μs , 3.9 μs , respectively. Compared with ERP accuracy based on solely 10 global stations, the improvement reaches 66.8%, 74.0%, 62.1%, respectively. The accuracy is equivalent to that of using 115 global stations.

The RMS of polar X, Y coordinate and LOD after introducing BDS-3 ISL are 25.6 μs , 21.0 μs , 3.9 μs , respectively. Compared with ERP accuracy based on solely 10 global stations, the improvement reaches 18.2%, 49.4%, 62.1%, respectively.

- 2) On the basis of 10 Chinese stations, the RMS of polar X, Y coordinate and LOD with 72 LEO satellites are 48.1 μs , 81.6 μs , 9.0 μs , respectively. Compared with ERP accuracy with solely ground stations, the improvement reaches 77.8%, 66.2%, 85.5%, respectively.

The RMS of polar X, Y coordinate and LOD after introducing BDS-3 ISL are 16.3 μs , 39.8 μs , 7.9 μs , respectively. Compared with ERP accuracy based on solely ground stations, the improvement reaches 92.5%, 39.8%, 87.3%, respectively. Since simulations ignore influences of unexpected error sources, our results would be more optimistic than actual cases.

With an overview of ERP estimations based on 10 Chinese stations, we found that the polar Y coordinate accuracy was always worse than that of X coordinate. This phenomenon was also observable in results of Wan et al. [9] that were based on measured GPS data from 18 Asia-Pacific stations. Since the longitude range of China varies from 73°E to 135°E, the polar X-axis points to the 0° meridian and the Y-axis points to the 270° meridian, the Chinese region is located on the same side of the polar X-axis. The regional distribution of the ground network would shift the polar coordinate estimation to one side of the Y direction.

Moreover, our correlation analysis between estimated orbit elements and ERP indicated that observations of LEO satellites and BDS-3 ISL reduce the correlation between the estimated parameters and thus improve the strength of normal equations. This fact could illustrate the contribution of LEO satellites and BDS-3 ISL on ERP accuracy improvement.

Acknowledgement. This work was sponsored by the National Key Research and Development Program of China (Project No.2020YFB0505601), National Natural Science Foundation of China (Grant No. 41931075, 41804024).

References

1. Beutler, G., Rothacher, M., Schaer, S., Springer, T.A., Kouba, J., Neilan, R.E.: The International GPS Service (IGS): an interdisciplinary service in support of earth sciences. *Adv. Space Res.* **23**(4), 631–653 (1999)
2. Rothacher, M., Beutler, G., Weber, R., Hefty, J.: High-frequency variations in earth rotation from global positioning system data. *J. Geophysical Res. Solid Earth* **106**(B7), 13711–13738 (2001)

3. Marshall, J.A., Lerch, F.J., Luthcke, S.B., Williamson, R.G., Chan, J.C.: An assessment of TDRSS for precision orbit determination. *J. Astronautical Sci.* **44**(1), 115–127 (1996)
4. Zhu, S., Reigber, C., König, R.: Integrated adjustment of CHAMP, GRACE, and GPS data. *J. Geodesy* **78**(1–2), 103–108 (2004)
5. Svehla, D.: Reference Frame from the Combination of a LEO Satellite with GPS Constellation and Ground Network of GPS Stations. In: *Geometrical Theory of Satellite Orbits and Gravity Field*. ST, pp. 29–41. Springer, Cham (2018). https://doi.org/10.1007/978-3-319-76873-1_2
6. Glaser, S., Michalak, G., König, R., Männel, B., Schuh, H.: Future GNSS Infrastructure for Improved Geodetic Reference Frames. In: *2020 European Navigation Conference (ENC)*, pp. 1–10 (2020)
7. Michalak, G., Glaser, S., Neumayer, K.H., König, R.: Precise orbit and earth parameter determination supported by LEO satellites, inter-satellite links and synchronized clocks of a future GNSS. *Adv. Space Res.* **68**(12), 4753–4782 (2021)
8. Noack, T., Engler, E., Klisch, A., Becker, C.: Statistical GNSS performance assessment as part of the ALEGRO Ground Based Augmentation System inside Research Harbour Rostock. In: *XIII International Scientific & Technical Conference on Marine Traffic Engineering.*, DLR (2009)
9. Wan, L., Wei, E., Jin, S.: Earth Rotation Parameter Estimation from GNSS and Its Impact on Aircraft Orbit Determination. In: *Proceedings of China Satellite Navigation Conference (CSNC) 2014*, pp. 105–114. Springer, Nanjing, China (2014)
10. Wang, Q., Dang, Y., Xu, T.: The Method of Earth Rotation Parameter Determination Using GNSS Observations and Precision Analysis. In: *Proceedings of China Satellite Navigation Conference (CSNC) 2013*, pp. 247–256. Springer, Wuhan, China (2013)